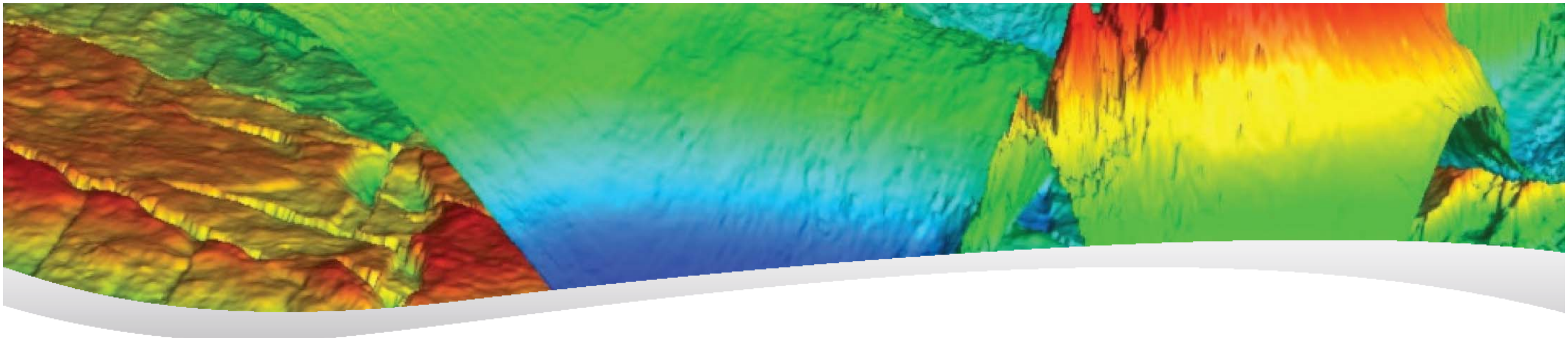

New Edge Detection Methods for Seismic Interpretation

Brian Russell and Claude Ribordy

CREWES

HAMPSON-RUSSELL
A CGG Company

Introduction

- In this talk, we discuss a set of edge enhancement methods for seismic data that involve derivatives of the seismic volume in the time, inline and cross-line directions.
- These methods were initially applied to potential field data for edge enhancement.
- Similar algorithms have been proposed for seismic edge detection, involving spatial differences between traces.
- The difference in these new approaches is the way in which the vertical derivative is used in the computation.
- The methods discussed here are also similar to coherency and curvature methods for seismic discontinuity detection.
- The methods will be illustrated using a structurally complex seismic volume recorded in the North Sea.

The derivative of a Gaussian in distance

- Let us first look at the effect of the derivative operation on a Gaussian function in time or distance:

$$g(t \text{ or } x) = A\exp\left(-\frac{(t \text{ or } x)^2}{\sigma^2}\right) \quad \Rightarrow \quad \frac{dg(t \text{ or } x)}{d(t \text{ or } x)} = -2A\frac{(t \text{ or } x)}{\sigma^2}\exp\left(-\frac{(t \text{ or } x)^2}{\sigma^2}\right)$$

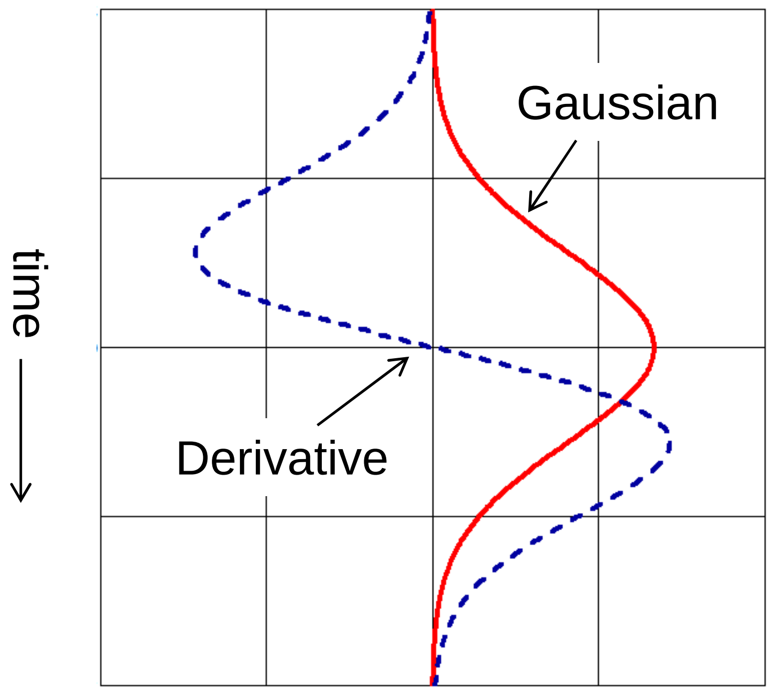

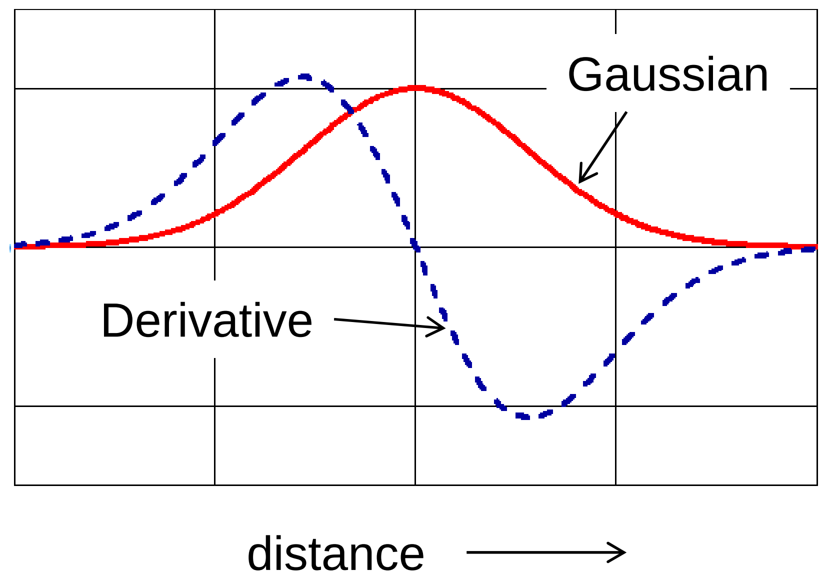

- Note that the Gaussian derivative has an extra zero crossing which creates a discontinuity, or turns peaks into edges.

Differentiation in the frequency domain

- A single frequency: $f(t) = \exp(i\omega t) = \cos(\omega t) + i\sin(\omega t)$
- Its derivative: $$\frac{df(t)}{dt} = i\omega\exp(i\omega t) = \omega\sin(\omega t) - i\omega\cos(\omega t)$$
- Note that differentiation increases the frequency content of a signal by multiplying it by ω and rotates its phase by 90°.

Amplitude and phase spectra of a Gaussian (solid red) and its derivative (dashed blue).

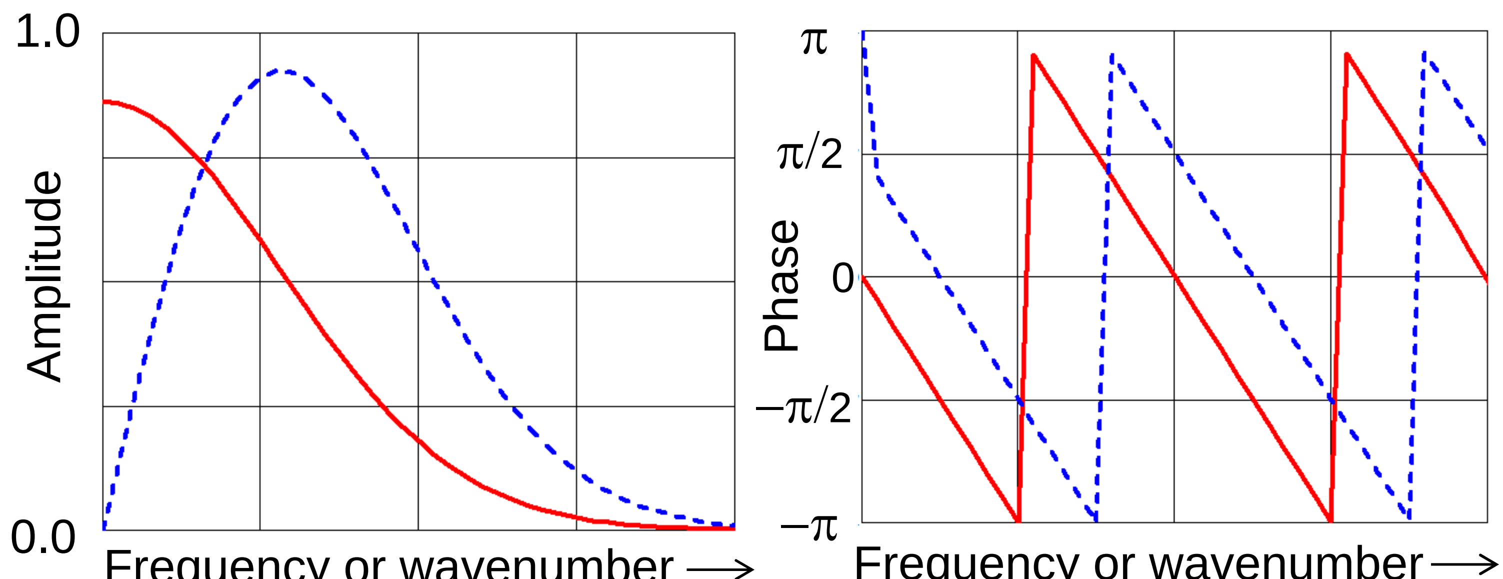

A history of edge detection

- Luo et al. (1996) proposed use differences between seismic traces to perform edge detection.
- The differencing can be thought of as applying a two point convolution operator:

$$d = \frac{1}{2}\left(1, -1\right)$$

- This filter can be applied in the inline or cross-line direction, or in a “star” pattern to average both directions.
- The results from Luo et al. (1996) are shown on the next slide.

Edge detection by differences

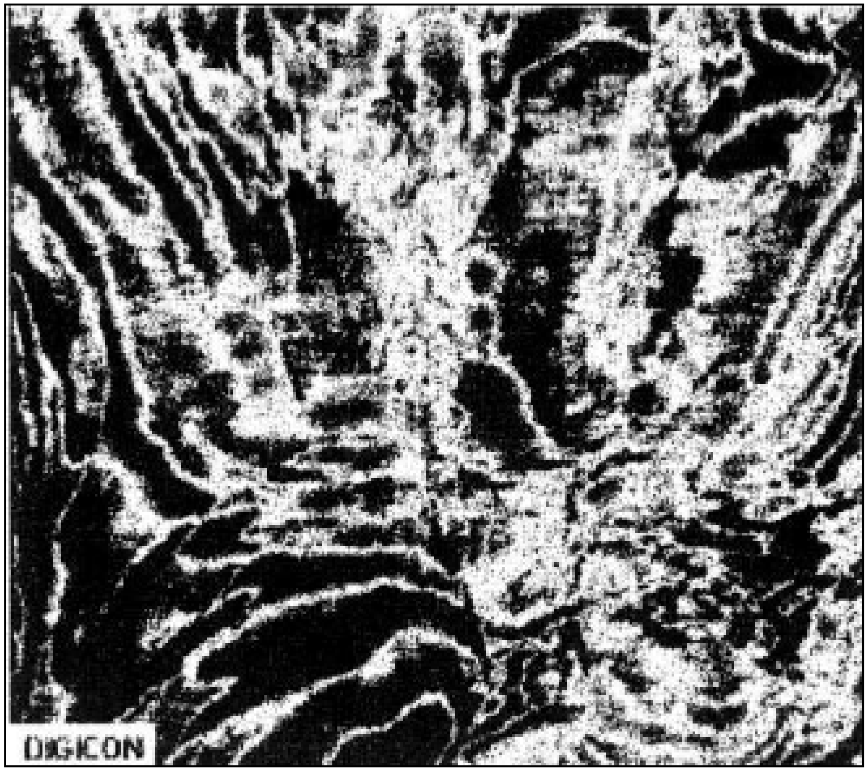

A slice from the input seismic section used in the study.

The difference cube shows a number of faults but is blurry.

Luo et al. (1996)

The effect of different filters

- al-Dossary et al. (2003) consider the effect of three different filter implementations.
- They tested these filters on the input shown at the top of the figure.
- The simple derivative filter is second from top.
- The Canny filter, which involves convolution with a Gaussian, is third from the top.
- A filter based on the Green’s function is at the bottom.

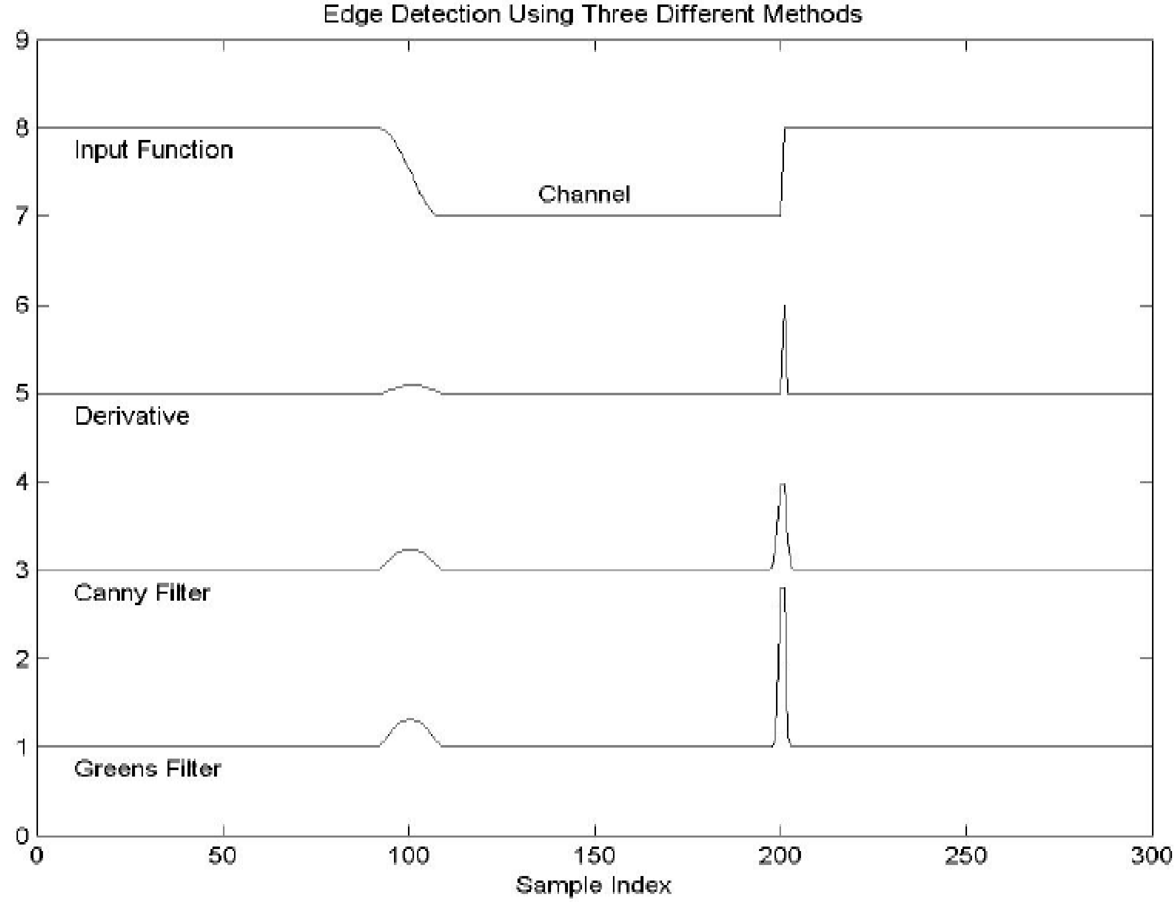

The effect of different filters

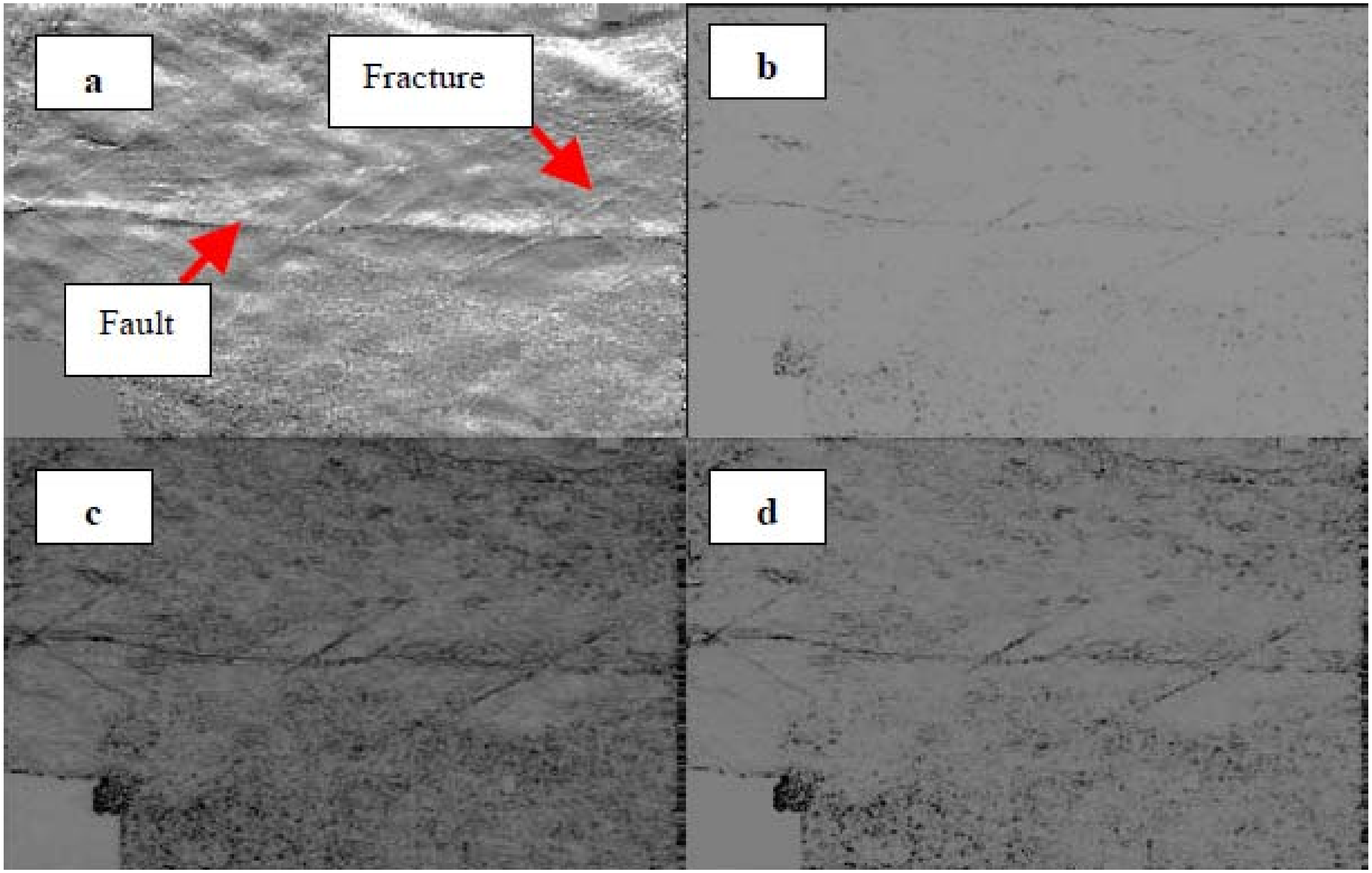

On noisy data, the type of derivative is important, where (a) shows the input, (b) the simple derivative, (c) the Canny derivative, and (d) the Green's function implementation. al-Dossary et al. (2003)

New derivative filters

- Cooper and Cowan (2008) review edge enhancement filters for potential field data based on combinations of derivatives in the $\boldsymbol{x}$, $\boldsymbol{y}$ and $\boldsymbol{z}$ directions.
- By changing from depth to time, we can implement these filters on seismic data.
- The seismic volume is a function of the 3 coordinates, or $\boldsymbol{f(x, y, t)}$**,** so we express these filters as partial derivatives:

$$f_x = \frac{\partial f(x,y,t)}{\partial x},\ f_y = \frac{\partial f(x,y,t)}{\partial y}, \text{and } f_t = \frac{\partial f(x,y,t)}{\partial t}.$$

- We found that implementing the simple two point derivative gave good results on the dataset used here.
- We now give a mathematical description of our four enhancement filters, and also of the coherency method.

The *TDX* filter

- Cooper and Cowan (2008) first define the *TDX* filter, or total horizontal derivative filter, which is mathematically equivalent to the square root of the Laplacian, or the absolute value of the gradient:

$$TDX = \left|\nabla f\right|_{xy} = \sqrt{\left(\frac{\partial f}{\partial x}\right)^2 + \left(\frac{\partial f}{\partial y}\right)^2}, \text{ where } \nabla f_{xy} = \begin{bmatrix} \dfrac{\partial f}{\partial x} \\ \dfrac{\partial f}{\partial y} \end{bmatrix} = \text{the 2D gradient.}$$

- Chopra and Marfurt (2012) also call this the Laplacian filter and show that it is equivalent to mean amplitude curvature.
- This filter is also identical to the Sobel filter used in photographic edge detection.

The tilt angle and its horizontal derivative

- Miller and Singh (1994) introduced the tilt angle filter into potential field measurements, by computing the arctangent of the vertical derivative divided by the Laplacian:

$$T = \arctan\left[\frac{\dfrac{\partial f}{\partial t}}{\sqrt{\left(\dfrac{\partial f}{\partial x}\right)^2 + \left(\dfrac{\partial f}{\partial y}\right)^2}}\right] = \arctan\left[\frac{\dfrac{\partial f}{\partial t}}{\left|\nabla f\right|_{xy}}\right]$$

- Verduzco et al. (2004) introduced the *THDR* filter, which is the (square root) Laplacian of the tilt angle:

$$THDR = \sqrt{\left(\frac{\partial T}{\partial x}\right)^2 + \left(\frac{\partial T}{\partial y}\right)^2}$$

The theta map

- Finally, Wijns et al. (2005) introduced the theta map, which is given by the ratio of the 2D and 3D (square root) Laplacian operators:

$$\cos\theta = \frac{\sqrt{\left(\frac{\partial f}{\partial x}\right)^2 + \left(\frac{\partial f}{\partial y}\right)^2}}{\sqrt{\left(\frac{\partial f}{\partial x}\right)^2 + \left(\frac{\partial f}{\partial y}\right)^2 + \left(\frac{\partial f}{\partial t}\right)^2}} = \frac{\left|\nabla f\right|_{xy}}{\left|\nabla f\right|_{xyt}},\ \text{where:}$$

$$\left|\nabla f\right|_{xyt} = \sqrt{\left(\frac{\partial f}{\partial x}\right)^2 + \left(\frac{\partial f}{\partial y}\right)^2 + \left(\frac{\partial f}{\partial t}\right)^2},\ \text{and } \nabla f_{xyt} = \begin{bmatrix} \frac{\partial f}{\partial x} \\ \frac{\partial f}{\partial y} \\ \frac{\partial f}{\partial t} \end{bmatrix} = \text{the 3D gradient.}$$

The coherency method

- The first coherency method involved finding the maximum correlation coefficients between adjacent traces in the x and y directions, and taking their harmonic average.
- Marfurt et al. (1998) extended this by computing the semblance of all combinations of J traces in a window.

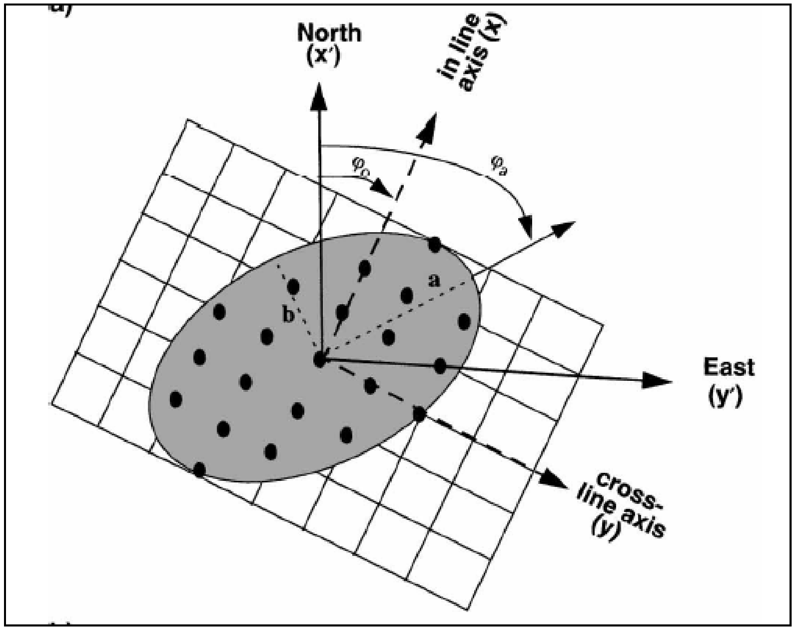

Marfurt et al. (1998)

- This involves searching over all x dips p and y dips q, over a $2M + 1$ sample window:

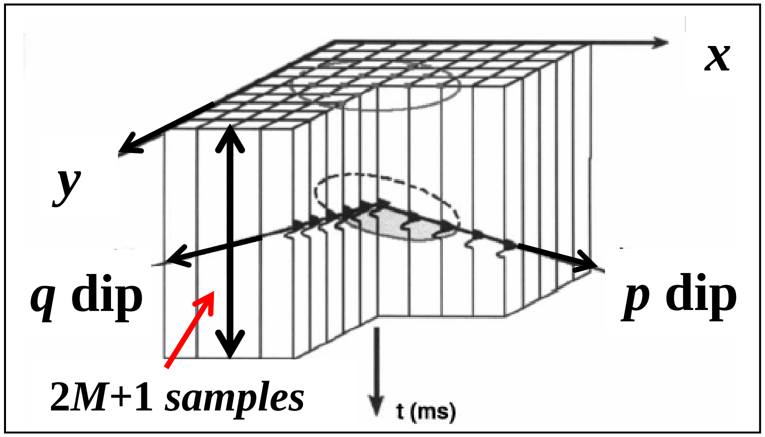

Model example

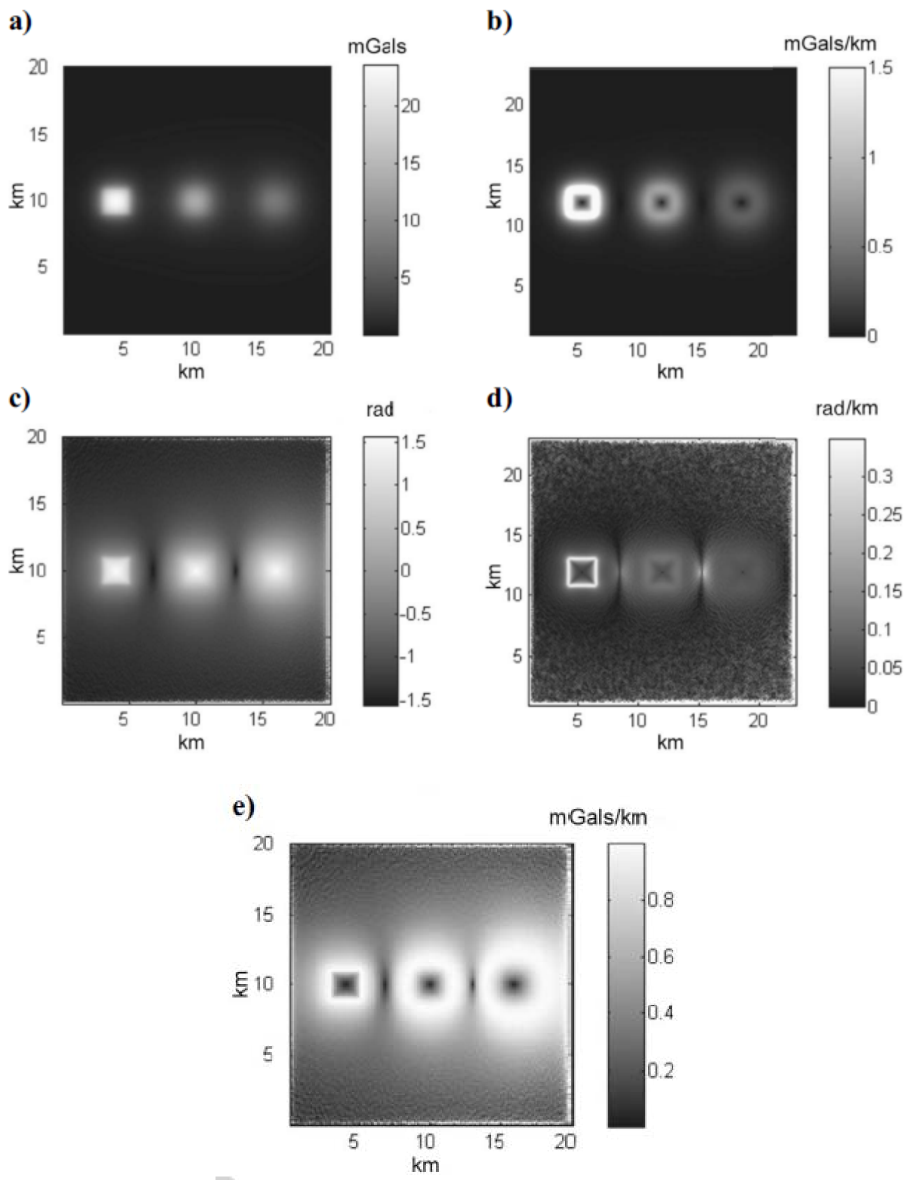

a) Cooper and Cowan (2008) show a synthetic gravity data set in a), consisting of anomalies from three identical cubic bodies with depths of 0.1, 0.5, and 1.1 km, with added random noise of 0.1%.

b) Total horizontal derivative of the data in a).

c) Tilt angle of the data in a).

d) THDR of the data in a).

e) Theta map of the data in a).

Real data tests

- The data used to test these algorithms is a subset of a structurally complex seismic volume over the F3 Block of the Netherlands portion of the North Sea.
- It has been graciously provided to us by Dr. Paul de Groot of dGB Earth Sciences.
- The dataset was pre-processed using the Insight Earth footprint removal workflow, which involved iterative footprint removal using five separate wavelength and azimuth orientations.
- “The most striking feature in this dataset is the large-scale sigmoidal bedding, with text-book quality downlap, toplap, onlap, and truncation structures.” (from the dGB OpenDetect training manual).

The F3 Block

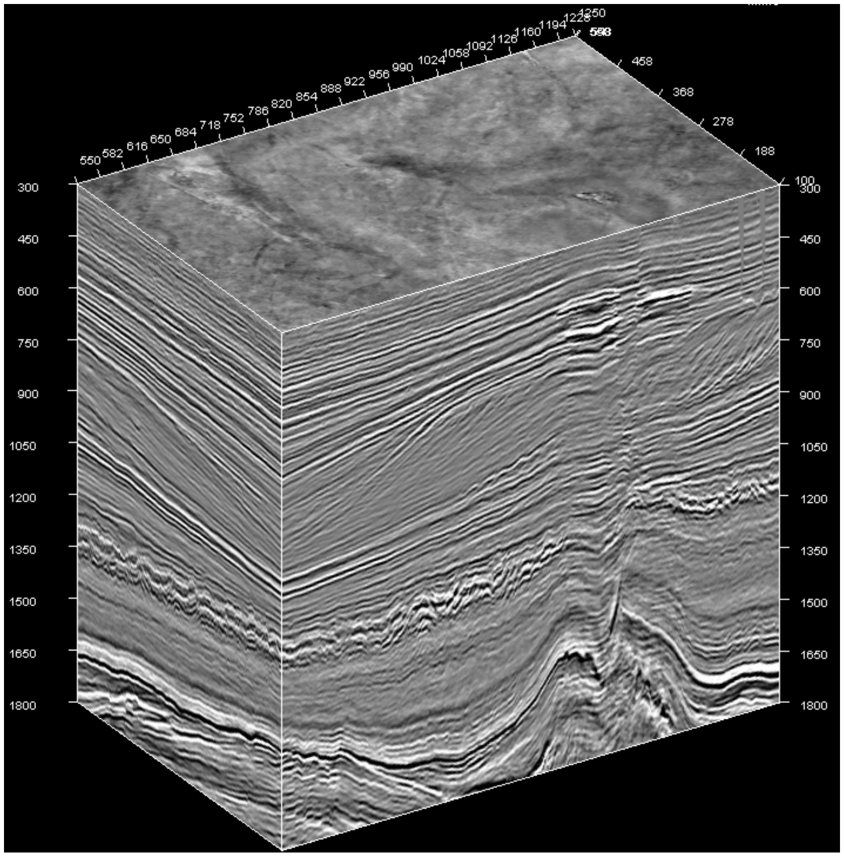

(a)

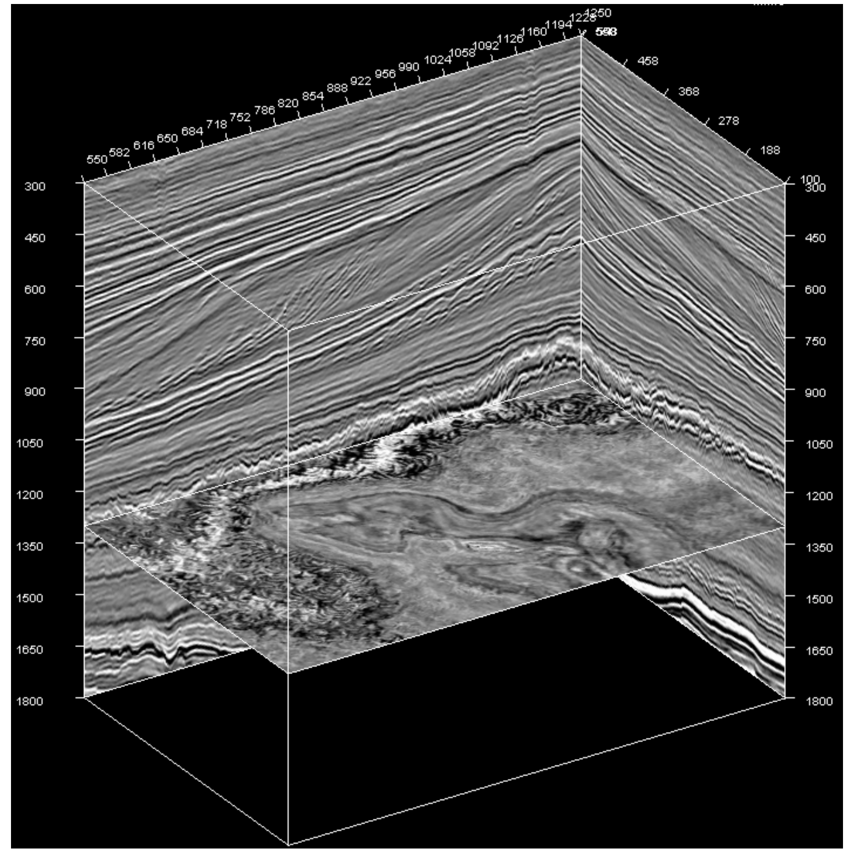

(b)

Three-dimensional images of the footprint-removed F3 seismic volume from the North Sea, where (a) shows the "outside" of the volume, and (b) shows the "inside" of the volume, with a time slice cut at 1300 ms.

Time Slice

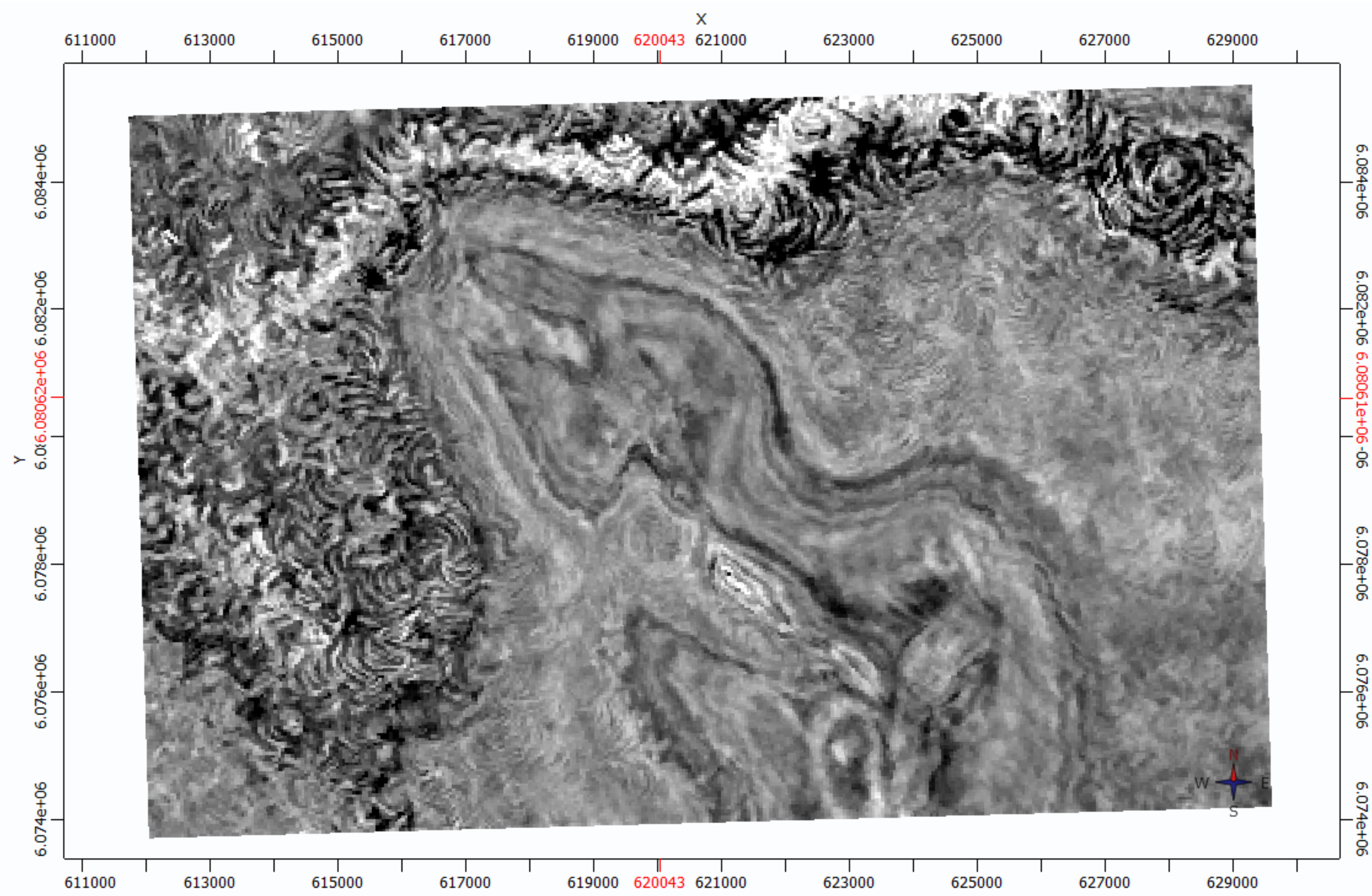

A map view of the time slice cut at a time of 1300 ms from the F3 volume. Note the variation in structures shown, from very small to very large.

The total horizontal derivative (*TDX*)

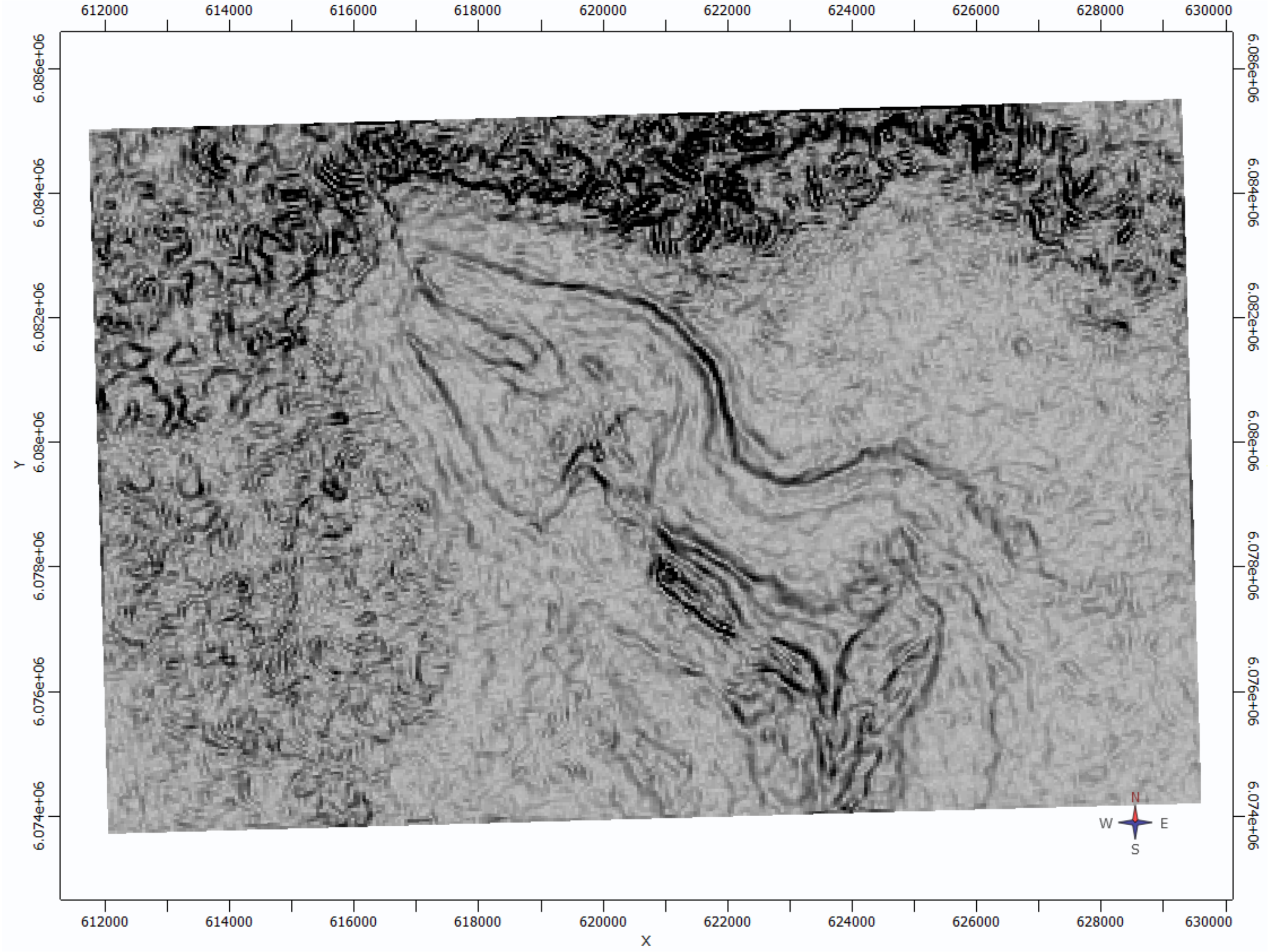

The application of the total horizontal derivative filter to the F3 volume and then time sliced at 1300 ms.

$$TDX = \sqrt{\left(\frac{\partial f}{\partial x}\right)^2 + \left(\frac{\partial f}{\partial y}\right)^2}$$

The tilt angle *T*

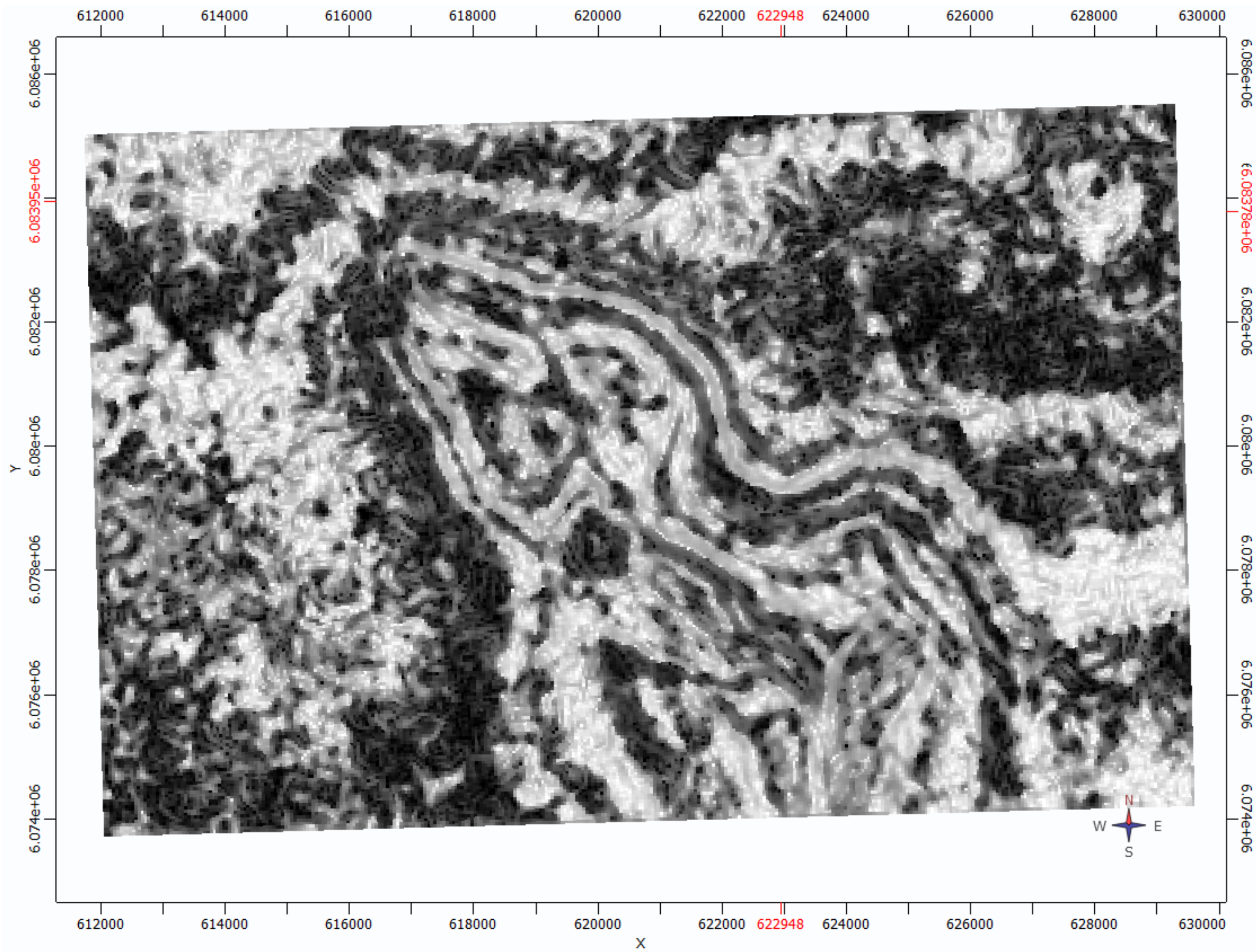

The application of the tilt angle filter to the F3 volume and then time sliced at 1300 ms.

$$T = \arctan\left[\frac{\partial f}{\partial t} / TDX\right]$$

Total horizontal derivative of tilt angle

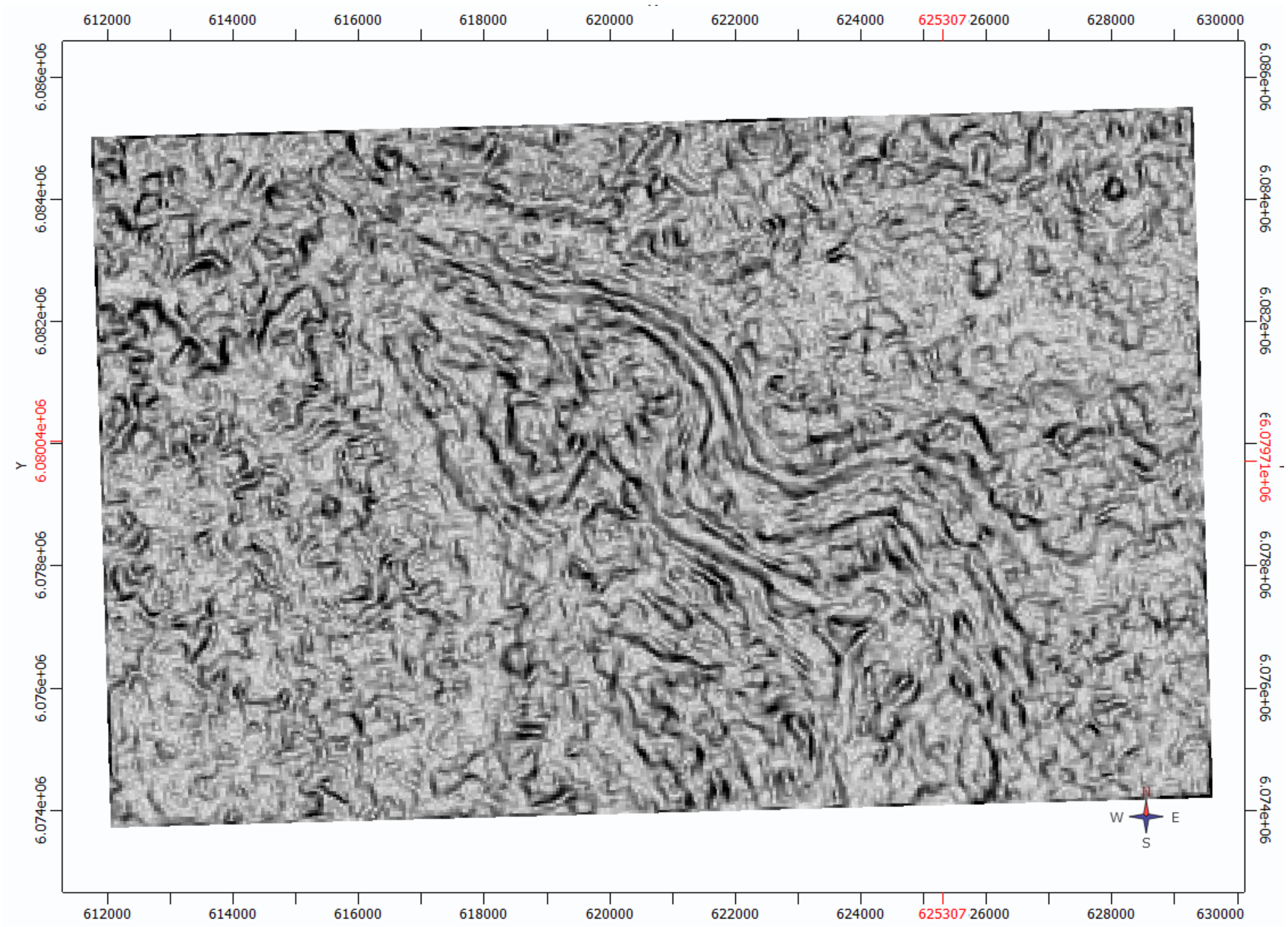

The application of the total horizontal derivative of the tilt angle, or *THDR*, filter to the F3 volume.

$$THDR = \sqrt{\left(\frac{\partial T}{\partial x}\right)^2 + \left(\frac{\partial T}{\partial y}\right)^2}$$

The theta map

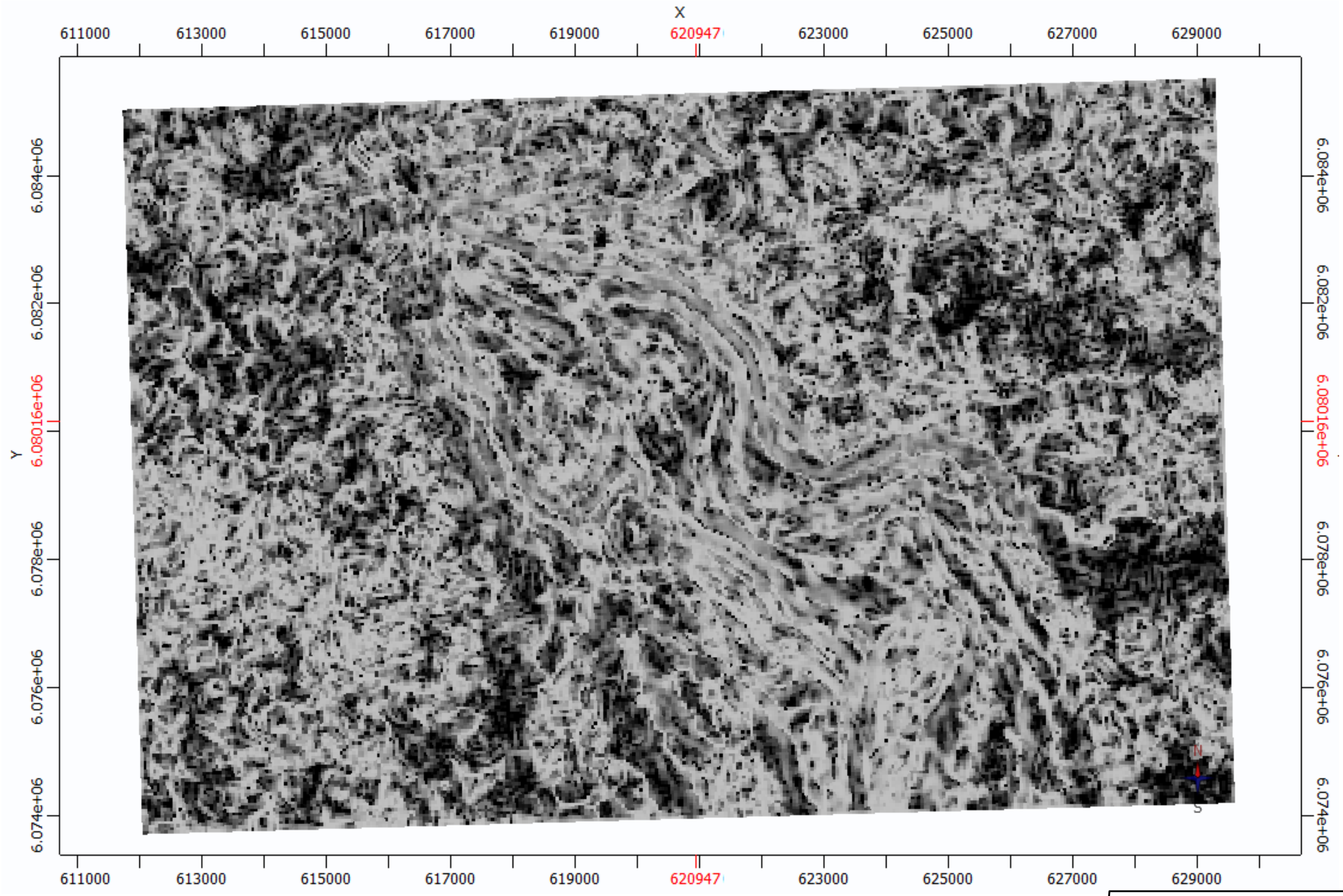

The application of the theta map to the F3 volume and then time sliced at 1300 ms.

$$\cos\theta = \frac{\sqrt{\left(\frac{\partial f}{\partial x}\right)^2 + \left(\frac{\partial f}{\partial y}\right)^2}}{\sqrt{\left(\frac{\partial f}{\partial x}\right)^2 + \left(\frac{\partial f}{\partial y}\right)^2 + \left(\frac{\partial f}{\partial t}\right)^2}}$$

Coherency applied to the F3 volume

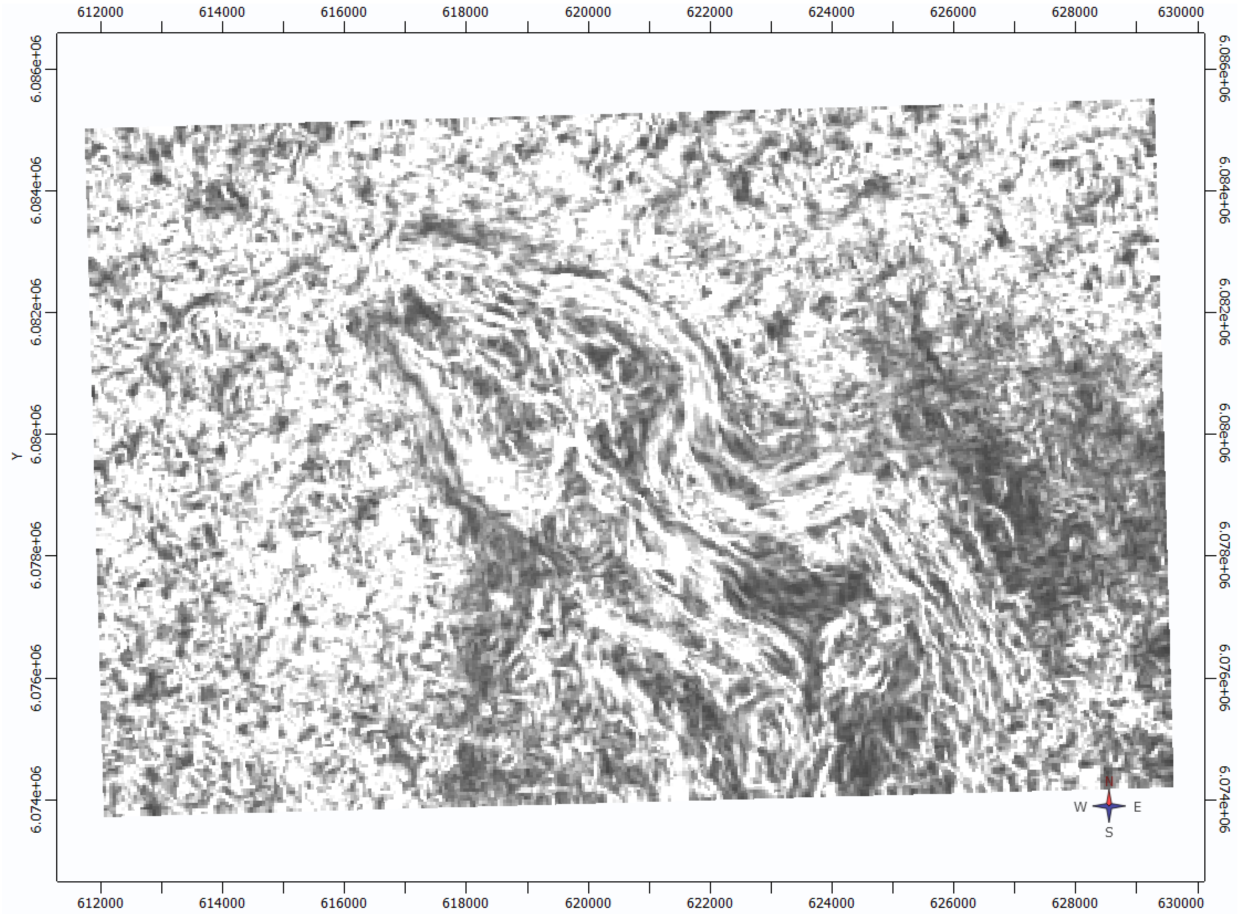

The application of the coherency method to the F3 volume and then time sliced at 1300 ms.

Conclusions

- We implemented a set of seismic edge detection methods for that were initially applied to potential field data.
- The methods were illustrated by a structurally complex seismic volume recorded in the North Sea.
- The total horizontal derivative, or Laplacian, method gave us a good indication of the edges of a time slice.
- The tilt angle method also produced good results, but less detailed than the total horizontal derivative.
- However, the total horizontal derivative of the tilt angle produced the most detailed picture of the structure.
- The theta map was not as detailed but showed the continuity of the structures very well.
- The coherency result also showed the continuity of the structures and was probably most close to the theta map.

Acknowledgements

I wish to thank the CREWES sponsors and my colleagues at Hampson-Russell, CGG, and CREWES.

In particular, I want to thank Joe Dominquez at Insight Earth in Denver for his application of their footprint removal algorithm.

References

al-Dossary, S., Marfurt K.J., and al-Binhassan, N., 2003, Comparative Study of Edge Detection Algorithms: SEG Technical Program Expanded Abstracts.

Canny, J., 1986, A computational approach to edge detection: IEEE Transactions on Pattern Analysis and Machine Intelligence, 8, 679-698.

Chopra, S. and K.J. Marfurt, 2012, Which curvature is right for you? Part 2: Presented at the 2012 CSPG/CSEG/CWLS GeoConvention.

Cooper, G.R.J, and Cowan, D.R., 2008, Edge enhancement of potential-field data using normalized statistics: Geophysics, **73**, no. 2, H1–H4.

Luo, Y., Higgs, W. G. and Kowalik, W.S., 1996, Edge detection and stratigraphic analysis using 3D seismic data: SEG Technical Program Expanded Abstracts.

Marfurt, K. J., R. L. Kirlin, S. H. Farmer, and M. S. Bahorich, 1998, 3D seismic attributes using a running window semblance-based algorithm: Geophysics, **63**, 1150–1165.

Miller, H. G., and V. Singh, 1994, Potential field tilt — A new concept for location

Torreao, J.R.A. and Amaral, M.S., 2002, Signal differentiation through a Torreao and Amaral's function approach: Parrtern Recognition Letters, 23, 1755-1759.

Verduzco, B., J. D. Fairhead, C. M. Green, and C. MacKenzie, 2004, The meter reader—New insights into magnetic derivatives for structural mapping: The Leading Edge, **23**, 116–119.

Wijns, C., C. Perez, and P. Kowalczyk, 2005, Theta map: Edge detection in magnetic data: Geophysics, **70**, no. 4, L39–L43.